化学气相沉积法低温制备氢气和多壁碳纳米管

刁金香[1],王惠[2]
(1.西安航空职业技术学院 航空维修工程学院,陕西 西安 710089;2.西北大学 合成与天然功能分子化学教育部重点实验室/化学与材料科学学院,陕西 西安 710069)

摘 要:采用低温化学气相沉积法裂解乙醇协同制备氢气和多壁碳纳米管,乙醇作为碳源,Ni/C 用作催化剂。考察反应温度和 Ni/C 比例对氢气的产率和碳纳米管品质的影响。多壁碳纳米管结构与组成通过扫描电镜、投射电镜和 X 射线粉末衍射进行表征。结果表明:Ni/C 催化剂最佳 Ni 担载量为 8%,最佳的反应温度为 500 ℃,最佳条件下氢气的产率为 79%,碳纳米管的品质最佳。

关键词:Ni/C 催化剂;多壁碳纳米管;制备
中图分类号:O613.71 **文献标识码**:A **文章编号**:1001-3741(2020)04-22-05
DOI:10.14078/j.cnki.1001-3741.2020.04.005

Low temperature preparation of hydrogen and multi-walled carbon nanotubes by CVD

Diao Jin-xiang[1], Wang Hui[2]
(1.School of Aviation Maintenance Engineering , Aeronautical Polytechnic Institute,Shaanxi Xi'an 710089,China;2. Key Laboratory of Synthetic and Natural Functional Molecule Chemistry (Ministry of Education), College of Chemistry & Materials Science, Northwest University,Shaanxi Xi'an 710069,China)

Abstract: Hydrogen and multi-walled carbon nanotubes (MWCNTs) were synthesized by low-temperature thermal chemical vapor deposition with ethanol as carbon sources and Ni/C as catalyst. The effects of the ratio of Ni to C and reaction temperatures on ethanol decomposition were investigated systematically. The structure and composition of the achieved MWCNTs products were studied by scanning and transmission electron microscope (SEM and TEM) as well as Raman and X-ray diffraction. The results indicate that Ni/C mass ration of 8% is the most effective catalyst for ethanol decomposition into hydrogen (the maximum H_2 yield of 79%) and multi-walled carbon nanotutes at 500 ℃.

Key words: Ni/C catalysts;multi-walled carbon nanotubes;hydrogen

为了将碳纳米管（CNT）与现有材料和技术整合，在基材上直接生长定向的 CNT 膜是一种实用、经济高效的方法,然而此方法的瓶颈问题是需要的高温与许多材料不兼容[1-5]。采用化学气相沉积法和等离子体增强的化学气相沉积法制备多壁碳纳米管的温度在 600~800 ℃[6-8]。低于 600 ℃制备碳纳米管已有报道,例如采用等离子体增强的化学气相沉积法制备碳纳米纤维/碳纳米管，催化剂为 Ni,Fe,Fe-Mo[9-14]和 $Ni_{0.67}$-Fe_{033}[15],碳源 C_2H_2/NH_3 和 C_2H_2[16-17]。

氢气是绿色清洁的能源，可用于 H_2-O_2 燃料电池。主要通过天然气蒸气转化的方法制备氢气,此方法的工艺复杂且成本高。目前,催化裂解含碳化合物(CH_4,CH_3OH,C_2H_2)制备氢气由于其副产物少而得到一定应用。乙醇因为低毒,来源广泛可以同时作为碳源和氢源引起了广泛的关注。本文采用镍金属作为催化剂,以石墨为担载体,研究了反应温度(400~700 ℃)、催化剂担载量对氢气产率和碳纳米管的催化性能影响。所得的气体产物采用气相色谱进行分析，固体产物组分和结构采用 XRD、Raman、SEM 和 TEM 进行分析。

1 实验

1.1 试剂和设备

硝酸镍（$Ni(NO_3)_2\cdot 6H_2O$），石墨(18.3 μm),无水乙醇(C_2H_5OH)。

扫描电子显微镜(Quanta 400 FEG);透射电子

基金项目：国家自然基金（No5130220,No516320075 和 No16722185),陕西省自然基金(No2019JM-080)，陕西省教育厅科研计划项目 (18JK0413)，西安航空职业技术学院 (18XHZY-019)

作者简介:刁金香(1983-),硕士研究生,副教授,在读博士,研究方向：碳纳米管/石墨复合材料的制备及其在锂离子电池应用研究、二维纳米杂化结构材料的自组装及其功能化研究。

收稿日期:2020-02-29

显微镜(JEOL JEM-3010);拉曼光谱仪(ALMEGA);X 射线粉末衍射仪(Rigaku RINT 2500V);催化剂评价装置 (WFSM-3011);大功率磁力搅拌器 (88-1);气相色谱仪 (SP-9890)。

1.2　Ni/C 催化剂的制备

将一定量的硝酸镍 $Ni(NO_3)_2 \cdot 6H_2O$ 溶解在一定量蒸馏水中,缓慢加入 1 g 担载体石墨(18.3 μm),室温下搅拌 24 h,得到均一的溶液。蒸发溶剂,在烘箱中 70 ℃ 干燥 12 h。将固体产物进行研磨,过筛,置于马弗炉煅烧, 在温度 350 ℃下煅烧 3 h,得到催化剂的前驱体。将 200 mg 的前驱体置于石英管的恒温部分, 在温度为 500 ℃,H_2 气氛下还原 1 h 得到催化剂。催化剂 Ni/C 的担载量以 Ni 的质量分数($[m_{Ni}/(m_{Ni}+m_C)]\times100\%$)表示,制备担载量为 2%、5%和 8%的催化剂,分别标记为 Ni(2%)/C、Ni(5%)/C 和 Ni(8%)/C。

1.3　氢气和多壁碳纳米管制备

乙醇裂解反应装置为 WFSM-3011 催化剂评价装置: 将上述石英管中的不同担载量的催化剂,分别升温至 400,500,600,700 ℃, 待反应温度恒定后,用微量进样器注入(流速为 0.3 mL/h)无水乙醇,通过汽化器进入石英管进行反应。反应过程中的气体产物用 SP-9890 进行检测分析,每隔 12 min 取 1 次样品进行检测。确定反应过程中的气体产物中含有大量的 H_2,少量的 CO,微量的 CH_4 和 CO_2。反应中固体的产物采用 SEM、Raman 和 TEM 进行表征。Ni/C 催化剂通过氢气的产率、气体产物的选择性进行评价。氢气的产率(H_2 yield)、各种气体产物的选择性(x_i)[15]的计算方法如式(1)~(2):

$$H_2\ \text{yield}=\frac{\text{产生的氢气物质的量}}{\text{乙醇中理论含氢分子的物质的量}} \quad (1)$$

$$x_i=\frac{n_i}{n_{\text{total}}}\times100\% \quad (2)$$

式 (2) 中 n_i 为 H_2、CO、CH_4 和 CO_2 的物质的量,n_{total} 为 H_2、CO、CH_4 和 CO_2 的物质量的总和。

2　结果与讨论

2.1　反应温度和催化剂担载量对氢气产率的影响

图 1 显示了 Ni(2%)/C, Ni(5%)/C 和 Ni(8%)/C 乙醇催化裂解 H_2 产率随温度和反应时间的变化,可以明显看出,在 500 ℃时,H_2 的产率最大。对于图 1(a)Ni(2%)/C 和图 1(c)Ni(8%)/C 催化剂,氢气产率的顺序为 500 ℃> 600 ℃> 400 ℃> 700 ℃。对于图 1(b)Ni(5%)/C,氢气产率的顺序为 500 ℃> 600 ℃> 700 ℃> 400 ℃。在 500 ℃下,乙醇在 Ni(8%)/C 条件下最大 H_2 产率为 79%。在 500 ℃下,随着催化剂担载量的变化,H_2 产率变化为 Ni(8%)/C (79%) > Ni(5%)/C (68%)> Ni(2%)/C (55%) 。原因可能是在相对较低的温度(400 ℃)下,催化剂的活性位点较少,不利于乙醇分解生成 H_2。然而,在高温下,催化剂发生烧结和团聚的现象, 反应温度为 700 ℃时, 可能导致 Ni/C 催化剂失活。此外,在 600 ℃时,在每种催化剂上都观察到轻微的失活现象。实验结果表明:Ni(8%)/C 催化剂在 500 ℃的 H_2 产率达到 79%,高于报道的数据[18-19]。

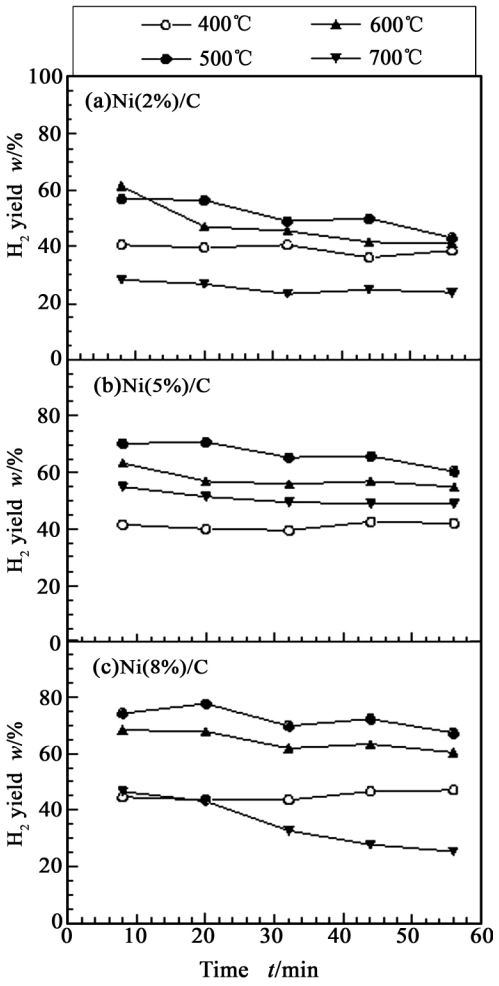

图 1　不同温度下乙醇在不同催化剂上裂解氢气产率随着时间的变化情况

Fig.1　Change of H_2 yield as a function of the reaction time in ethanol decomposition over Ni (2%, 5% and 8%)/C at different temperatures

图 2 显示了不同温度和担载量 Ni/C 催化剂在反应 60 min 后,各种气体选择性,除氢气外,还检测到一氧化碳、甲烷和二氧化碳。反应温度为 400~700 ℃时,其选择性(x_i)的变化顺序为 H_2>CO> CH_4> CO_2,这与热力学数据一致。反应温度为 500 ℃时,对于 Ni(2%)/C 和 Ni(5%)/C 催化剂,CO 的选择性约为 28%;Ni(8%)/C 的 CO 的选择性约为 21%。对于 Ni(8%)/C 催化剂 CH_4 和 CO_2 的选择性约为 5.2%和4.0%。此选择性与 H_2 的产率结果一致。

2.2　温度和催化剂担载量对碳纳米管的影响

图 3(a~c)为 500,600,700 ℃下 Ni(8%)/C 催化裂

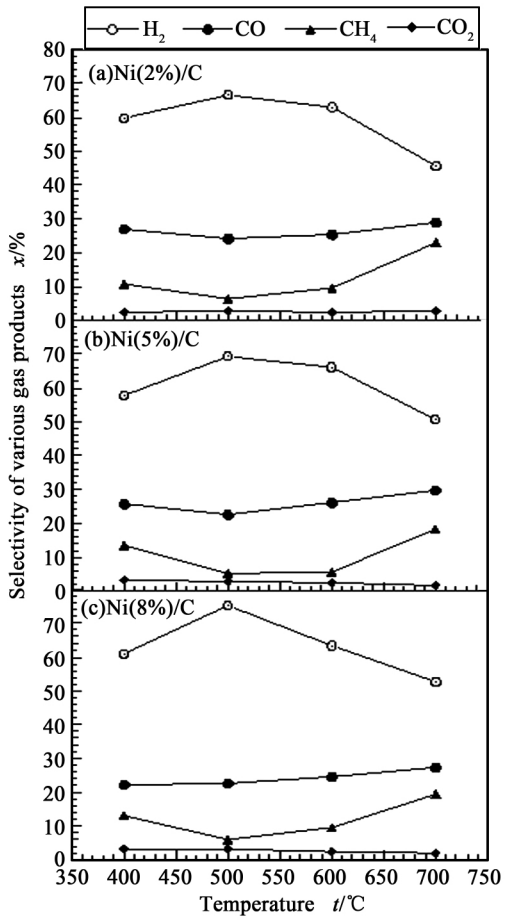

图 2 不同温度下 H_2,CO,CH_4 和 CO_2 的选择性

Fig.2 Change of selectivity of various gas as a function of the reaction temperature in ethanol decomposition over Ni (2%, 5% and 8%)/C at different temperatures

解 CNTs 的 SEM 图像。当温度为 500 ℃时,碳纳米管的管壁直,管径分布均匀,缠绕现象不明显,碳纳米管的品质较好;当温度上升到 600 ℃时,碳纳米管相互缠绕,在 SEM 图谱中看出有白色大的亮点为团聚的催化剂颗粒;当反应温度为 700 ℃时,催化剂发生团聚和烧结,生成了长短不均匀的炭纤维。图 3(d~e)为反应温度为 500 ℃时,Ni(2%)/C 和 Ni(5%)/C 催化裂解乙醇生长 CNTs 的 SEM 图,与 Ni(8%)/C 相比,碳纳米管的管径缠绕严重,同时出现了团聚的现象。结果表明:Ni/C 催化裂解乙醇制备碳纳米管最佳的反应温度为 500 ℃,最佳的担载量为 8%。同时对于 Ni(8%)/C 裂解乙醇的固体产物进行 XRD 分析,从图 3 (f) 看出,CNTs 的衍射峰 2θ=25.8°和 42.7°接近天然石墨的衍射峰。2θ=44.5°和 51.8°对应着 Ni 的(111)和(200) (PDF#65-0380)。

图 4(a)为反应温度 500,600 和 700 ℃下,乙醇在 Ni (8%)/C 发生裂解反应时生成的碳纳米管的 Raman 图。由图 4 (a) 可知,产物的 I_G/I_D 的顺序为 500 ℃(I_G/I_D=5.5)> 600 ℃ (I_G/I_D=3.0)> 700 ℃ (I_G/I_D=1.4)。结果表明,在 500 ℃时,制备的碳纳米管的品质最好。图 4(b)为反应温度为 500 ℃,Ni(2%)/C,Ni(5%)/C 和 Ni(8%)/C 催化裂解乙醇制备碳纳米管的拉曼光谱图。如图 4(b) 所示,I_G/I_D 随着担载量的升高而增加。当担载量为 8%时,I_G/I_D 最大,碳纳米管的品质最佳。因此,反应温度为 500 ℃,担载量为 8%时,碳纳米管的品质最佳。此结果与扫描电镜产氢

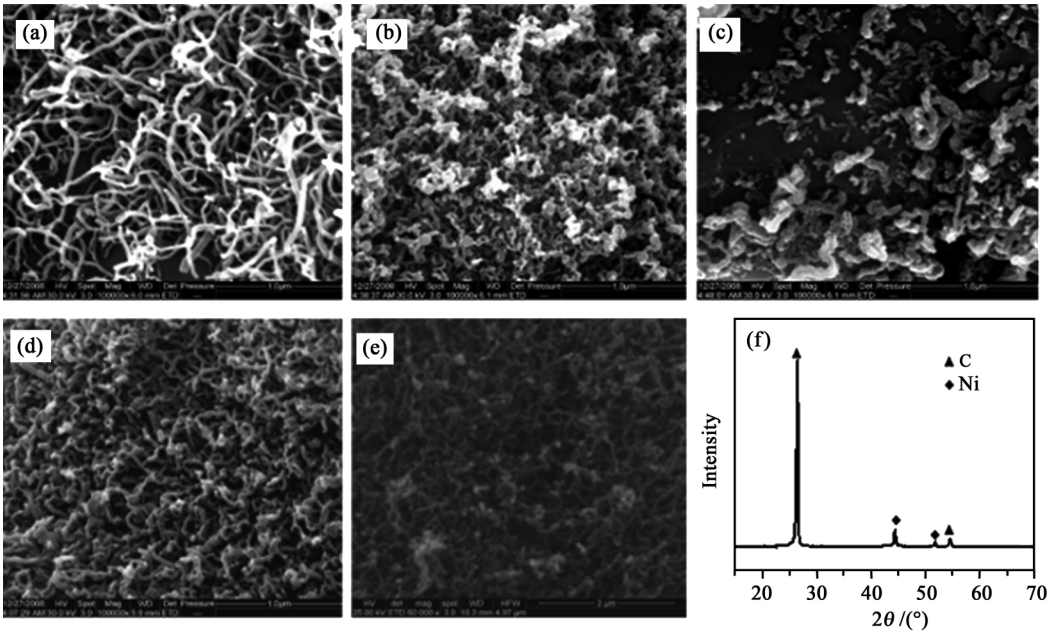

图 3 (a~c) 不同温度下 Ni(8%)/C 催化裂解乙醇制备碳纳米管 SEM 图;(d~e) 反应温度为 500 ℃,Ni(2%)/C 和 Ni(5%)/C 催化裂解乙醇制备碳纳米管的 SEM 图;(f) 500 ℃,Ni(8%)/C 裂解乙醇产物的 XRD 图

Fig.3 (a~c) SEM images of MWCNTs formed by the ethanol decomposition over the Ni(8%)/C at different temperatures of 500~700 ℃; (d~e) SEM images of MWCNTs formed by the ethanol decomposition over the Ni (2%)/C and Ni (5%)/C at the temperatures of 500 ℃; (f) XRD pattern of MWCNTs formed by ethanol decomposition over Ni(8%)/C catalyst at 500 ℃

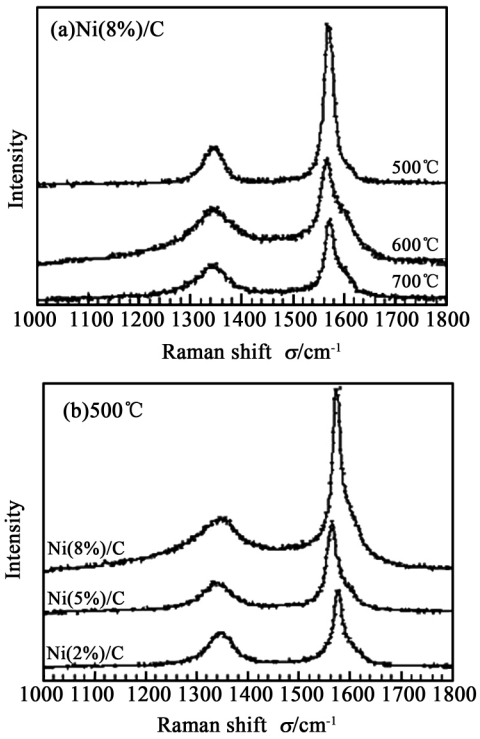

图 4　不同温度(a)不同催化剂担载量(b)下制备的碳纳米管拉曼光谱图

Fig.4　(a) Raman of MWCNTs formed by the ethanol decomposition over the Ni(8%)/C at different temperatures of 500~700 ℃;(b) Raman of MWCNTs formed by the ethanol decomposition over the Ni(2%)/C, Ni(5%)/C and Ni(8%)/C at the temperatures of 500 ℃

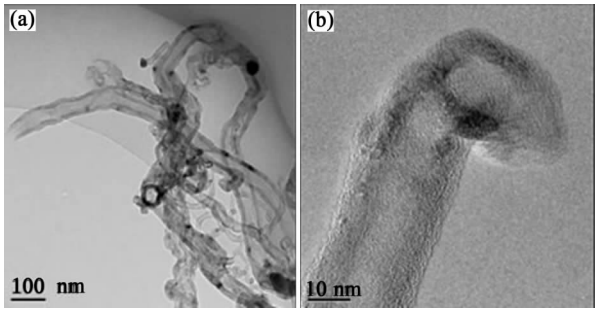

图 5　乙醇在 500 ℃时,Ni(8%)/C 催化剂上裂解生长的多壁碳纳米管的 TEM

Fig.5　TEM images of MWCNTs formed by ethanol decomposition over Ni(8%)/C catalyst at 500 ℃

结果一致。

图 5 为乙醇在 500 ℃时于 Ni(8%)/C 催化剂上裂解生长的多壁碳纳米管的 TEM 图。图中的黑色部分为催化剂颗粒,直径在 25~50 nm,如图 5(a)所示。碳纳米管的外径为 23 nm,内部直径为 8~10 nm,碳纳米管石墨层不清晰。碳纳米管的顶部黑色点生长如图 5(b)所示。

3　结论

研究了 Ni/C 催化裂解乙醇制备的氢气和碳纳米管,考察了反应温度和 Ni 担载量对氢气产率和碳纳米管质量的影响。最佳的反应温度为 500 ℃,最佳担载量为 8%,最佳条件下氢气的产率为 79%。所制备的碳纳米管为多壁碳纳米管,外径为 23 nm,内部直径为 8~10 nm。

参考文献:

[1] Mukhopadhyay K, Koshio A, Sugai T, et al. Bulk production of quasi-aligned carbon nanotube bundles by the catalytic chemical vapour deposition (CCVD) method[J]. Chemical Physics Letters, 1999, 303(1-2): 117-124.

[2] Ryu J E, Lee C J, Lee T J, et al. Growth of vertically aligned carbon nanotubes on Co-Ni alloy metal [J]. The Transactions of the Korean Institute of Electrical Engineers C, 2000, 49(8): 451-454.

[3] Fleming E, Du F, Ou E, et al. Thermal conductivity of carbon nanotubes grown by catalyst-free chemical vapor deposition in nanopores[J]. Carbon, 2019, 145: 195-200.

[4] Ahmad S, Liao Y, Hussain A, et al. Systematic investigation of the catalyst composition effects on single-walled carbon nanotubes synthesis in floating-catalyst CVD[J]. Carbon, 2019, 149: 318-327.

[5] Tzounis L, Liebscher M, Fuge R, et al. P and n-type thermoelectric cement composites with CVD grown p-and n-doped carbon nanotubes: Demonstration of a structural thermoelectric generator [J]. Energy and Buildings, 2019, 191: 151-163.

[6] Gautier L A, Le Borgne V, El Khakani M A. Field emission properties of graphenated multi-wall carbon nanotubes grown by plasma enhanced chemical vapour deposition[J]. Carbon, 2016, 98: 259-266.

[7] Shaukat S, Khaleeq-ur-Rahman M, Dildar I M, et al. Aerosol assisted chemical vapor deposition (AACVD) synthesis of nanostructured cauliflower patterning in MWCNT doped tungsten oxide[J]. Ceramics International, 2019, 45 (2): 1918-1927.

[8] Mubarak N M, Sahu J N, Abdullah E C, et al. Rapid adsorption of toxic Pb (II) ions from aqueous solution using multiwall carbon nanotubes synthesized by microwave chemical vapor deposition technique [J]. Journal of Environmental Sciences, 2016, 45: 143-155.

[9] Shen Y, Gong W, Zheng B, et al. Ni-Al bimetallic catalysts for preparation of multiwalled carbon nanotubes from polypropylene: Influence of the ratio of Ni/Al [J]. Applied Catalysis B: Environmental, 2016, 181: 769-778.

[10] Arunkumar T, Karthikeyan R, Ram Subramani R, et al. Synthesis and characterisation of multi-walled carbon nanotubes (MWCNTs)[J]. International Journal of Ambient Energy, 2018: 1-5.

[11] Panic S, Bajac B, Rakic S, et al. Molybdenum anchoring effect in Fe-Mo/MgO catalyst for multiwalled carbon nan-

otube synthesis [J]. Reaction Kinetics, Mechanisms and Catalysis, 2017, 122(2): 775–791.

[12] Kim P, Lee C J. The reduction temperature effect of Fe–Co/MgO catalyst on characteristics of multi–walled carbon nanotubes[J]. Catalysts, 2018, 8(9): 361.

[13] Dubey P, Choi S K, Choi J H, et al. High–quality thin–multiwalled carbon nanotubes synthesized by Fe–Mo/MgO catalyst based on a sol–gel technique: synthesis, characterization, and field emission [J]. Journal of Nanoscience and Nanotechnology, 2010, 10(6): 3998–4006.

[14] Ramakrishnan S, Jelmy E J, Dhakshnamoorthy M, et al. Synthesis of carbon nanotubes from ethanol using RF–CCVD and Fe–Mo catalyst [J]. Synthesis and Reactivity in Inorganic, Metal–Organic, and Nano–Metal Chemistry, 2014, 44(6): 873–876.

[15] Chiang W H, Sankaran R M. Synergistic effects in bimetallic nanoparticles for low temperature carbon nanotube growth[J]. Advanced Materials, 2008, 20(24): 4857–4861.

[16] Ali J, Kumar A, Husain S, et al. Characterization and field emission studies of uniformly distributed multi–walled carbon nanotubes (MWCNTs) film grown by low–pressure chemical vapour deposition (LPCVD)[J]. Current Nanoscience, 2011, 7(3): 333–336.

[17] Fraga M A, Pessoa R S, Barbosa D C, et al. One–dimensional carbon nanostructures—from synthesis to nano–electromechanical systems sensing applications[J]. Sensors and Materials, 2017, 29(1): 39–56.

[18] Wang G, Wang H, Tang Z, et al. Simultaneous production of hydrogen and multi–walled carbon nanotubes by ethanol decomposition over Ni/Al_2O_3 catalysts[J]. Applied Catalysis B: Environmental, 2009, 88(1–2): 142–151.

[19] Ahmed W, El–Din M R N, Aboul–Enein A A, et al. Effect of textural properties of alumina support on the catalytic performance of Ni/Al_2O_3 catalysts for hydrogen production via methane decomposition[J]. Journal of Natural Gas Science and Engineering, 2015, 25: 359–366.

[上接第 16 页]

[25] Yi S J, Fan Z, Wu C, et al. Catalytic graphitization of furan resin carbon by yttrium [J]. Carbon, 2008, 46: 378–380.

[26] Yi S J, Chen J H, Xiao X, et al. Effect of praseodymium on catalytic graphitization of furan resin carbon [J]. Journal of Rare Earths, 2010, 28(1): 69–71.

[27] 齐静. 直接甲醇燃料电池电催化剂及新型碳载体的研究[D]. 大连: 中国科学院大连化学物理研究所, 2011.

[28] 张玉艳. 燃料电池阴极过渡金属碳基催化剂设计与制备[D]. 大连: 大连理工大学, 2016.

[29] Becke A D. Density functional thermochemistry. III. The role of exact exchange [J]. The Journal of Chemical Physics, 1993, 98(7): 5648–5652.

[30] Miehlich B, Savin A, Stoll H, et al. Results obtained with the correlation energy density functionals of Becke and Lee, Yang and Parr [J]. Chemical Physics Letters, 1989, 157(3): 200–206.

[31] Nielson K D, Van Duin A C T, Oxgaard J, et al. Development of the ReaxFF reactive force field for describing transition metal catalyzed reactions, with application to the initial stages of the catalytic formation of carbon nanotubes [J]. The Journal of Physical Chemistry A, 2005, 109(3): 493–499.

[32] Hay P J, Wadt W R. Ab initio effective core potentials for molecular calculations. Potentials for K to Au including the outermost core orbitals [J]. The Journal of Chemical Physics, 1985, 82:299–310.

[33] Xu S H, Zhang F Y, Kang Q, et al. The effect of magnetic field on the catalytic graphitization of phenolic resin in the presence of Fe–Ni [J]. Carbon, 2009, 47(14): 3233–3237.

[34] Strout D L, Hall M B. Structure and stability of lanthanum–carbon cations [J]. The Journal of Physical Chemistry A, 1998, 102(3):641–645.

[35] Strout D L, Hall M B. Small yttrium-carbon and lanthanum-carbon clusters:rings are most stable [J]. The Journal of Physical Chemistry, 1996, 100 (46):18007–18009.

[36] Sun X Y, Du J G, Jiang G. Au–doped carbon clusters AuC_n with n=1~11: a theoretical investigation [J]. Structural Chemistry, 2013, 24(4):1289–1295.